

Efficiency of maximum power point tracking in photovoltaic system under variable solar irradiance

W. MARAÑDA* and M. PIOTROWICZ

Department of Microelectronics and Computer Science, Lodz University of Technology, 221/223 Wólczańska St., 90-924 Łódź, Poland

Abstract. Field conditions decrease the energy output of photovoltaic (PV) systems, mainly due to excessive temperatures. However, in regions with moderate ambient temperatures, as in Poland, solar energy is commonly delivered with highly fluctuating irradiance. This introduces yet another source of energy losses due to the non-ideal tracking of actual position of Maximum Power Point (MPP).

Majority of PV-systems are equipped with DC/AC and grid-connected inverter. Since the solar energy flux is variable, an adequate MPP-tracking algorithm is required to handle a wide range of load levels and face rapid changes of input power. Along with the essential DC/AC conversion, the quality of MPP-tracking must also be taken into account in evaluation of inverter efficiency.

The tracking in dynamic conditions has been addressed only recently. Several algorithms has been studied theoretically, experimentally or in laboratory conditions by applying artificial input test-patterns. This work takes the opposite approach by applying the recorded real-life solar irradiance and simulating the tracking behavior to study the problem for true field conditions in Poland.

The simulation uses the unique high-quality irradiance data collected with 200 ms time resolution. The calculation of both static and dynamic MPP-tracking efficiency has been performed for representative variable-cloudy day, applying commonly used Perturb&Observe tracking algorithm.

Key words: photovoltaics, MPP-tracking, inverter efficiency.

1. Introduction

The conversion from solar radiant energy into AC-grid electricity in a photovoltaic (PV) system is a chain process consisting of many stages. All the stages contribute to the final yield with their efficiency. Only the thorough understanding of all-stages phenomena allows for accurate evaluation of conversion efficiency and assure the correct energy yield calculation.

The main factors contributing to energy losses in photovoltaic systems are the absence of Maximum Power Point tracking (up to 30% in respect to the offered maximum by PV-generator) and the excessive warming of PV-devices (up to 20%) [1], even in a moderate climate (up to 15% [2]).

Nowadays, in quest of maximization of total conversion efficiency in PV-systems, the attention is turned to study also the processes regarded as less significant in the past. Even the small improvements can bring substantial results when the large scale of their application is considered. The world-wide volume of installed photovoltaics is growing at an exponential rate for the last 10 years, exceeding the level of 100 GWp in 2012 and targeting 0.5 TWp before 2020 [3]. In the next decade, the PV-systems can become a major contributor to the idea of distributed energy generation, which will redefine many aspects of energy management in the global scale [4].

In Europe almost all PV-systems are connected to the utility grid and in majority located in variable-weather regions (mainly Germany, but also Benelux, Czech Rep. and Great Britain). The DC/AC PV-inverter is a key element in the con-

version chain in grid-connected systems. Apart from the essential DC/AC conversion, it is responsible for keeping the PV-generator in MPP to ensure the maximal energy production from the PV. The fluctuations of irradiance make the MPP to constantly change the positions, that must be followed by an adequate MPP-tracking algorithm. Therefore, the MPP-tracking issue is important for PV-systems operating in a great part of Europe.

However, the manufacturer specification for PV-inverter most often contain only the peak DC-AC efficiency or the graph of efficiency vs. load. This, however, is not enough for accurate energy yield forecast, especially in variable cloudy conditions, where the operation under highly fluctuating irradiance cannot be neglected.

In the past, several algorithms for MPP-tracking has been proposed, but only recently the tracking quality under variable irradiance has been acknowledged as relevant. The study on MPP-tracking have so far concentrated on the theoretical analysis of tracking algorithms under dynamic conditions and measurements of inverter responses to artificial input test-patterns in laboratories. The work to establish the formal standards for MPP-tracking quality measurements is also under way.

This paper focuses on detailed analysis of MPPT-tracking algorithm under true field conditions in Poland to answer to question of energy losses during variable-cloudy days due to imperfect tracking. This analysis has been performed by

*e-mail: maranda@dmcs.p.lodz.pl

means of simulation of PV-generator to compare the true positions of MPP with those obtained by tracking algorithm operation. The simulation has used a unique solar irradiance data recorded with 200 ms resolution, which makes the calculations very accurate.

The analysis has been performed for the representative day with highly variable irradiance and the fundamental and widely implemented Perturb&Observe MPP-tracking algorithm. The tracking process has been studied separately for steady and changing irradiance, i.e. for static and dynamic tracking, for several tracking-speed rates.

2. Recorded solar irradiance

The credibility of MPP-tracking analysis relies primarily on accurate irradiance data with sufficient time resolution. The data used in this article are being collected at the Solar Laboratory of Department of Microelectronics and Computer Science [5] since 2010 with 200 ms time interval.

The recording is performed with the fast photodiode-based SPLite pyranometer from Kipp&Zonen with the response time below 1 ms. The thermocouple-based sensors, although more accurate, could not be used due to the long response time (up to 5–10 s). The sensor is measuring the global irradiance in plane with 30° inclination towards south.

The sampling time of 200 ms assures that all irradiance fluctuations, relevant for MPP-tracking, are recorded. The fastest changes of irradiance are due to sharp cloud edges moving with strong wind. There are many cases of registered gradients exceeding 1000 W/m²/s. The experiment reveals the real variability of terrestrial irradiance, as shown in Fig. 1.

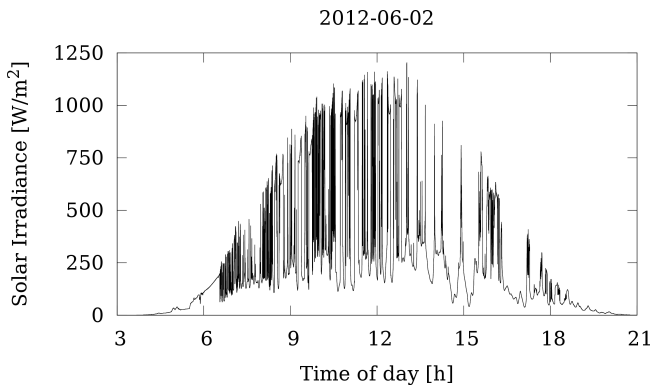


Fig. 1. Daily irradiance: 2012-06-02, Łódź

The commonly available irradiance measurements are averaged over several minutes, typically 15 or 30. They do not contain the variability information and are useless for tracking evaluation.

The high fluctuations of radiation flux are by no means exceptional in Polish climatic conditions. The collection of daily irradiance profiles, shown in Fig. 2, demonstrates the domination of variable-cloudy sunshine, especially in summer.

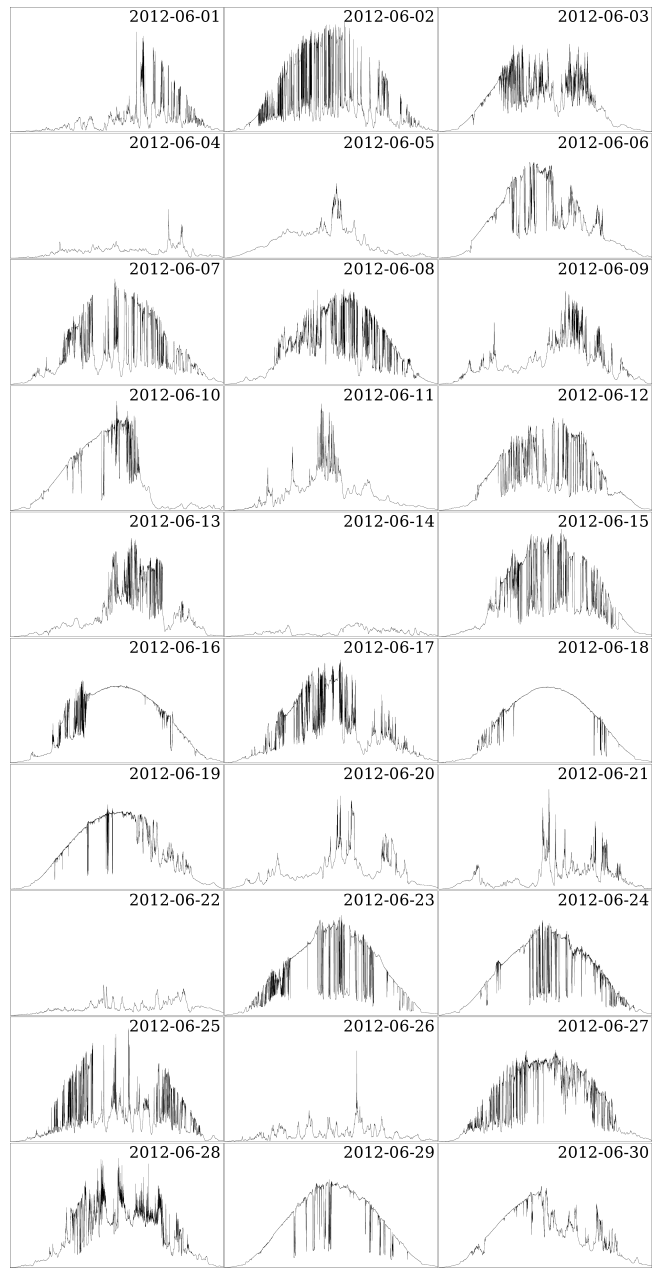


Fig. 2. Irradiance in June 2013, Łódź (axes as in Fig. 1)

3. Maximum Power Point under field conditions

A PV-device can be represented by an equivalent circuit as in Fig. 3. This approach guarantees sufficient accuracy for steady-state operation when the irradiance and temperature dependence coefficients are taken into account. The comprehensive review of modeling can be found in [6].

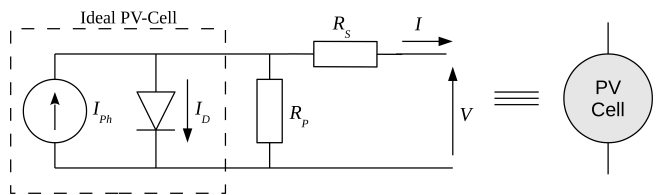


Fig. 3. Equivalent model of PV-cell

An arbitrary size PV-array may be formed by combining cells in serial and/or parallel chains (Fig. 4). The equivalent model still holds, but the element values must be corrected for the dimension of serial×parallel interconnection. The maximum power is delivered in MPP with V_{MPP} voltage and I_{MPP} current, as in Fig. 4. Driving the voltage (and current) close to MPP to maximize the energy output is thus the sole responsibility of the connected load (PV-inverter).

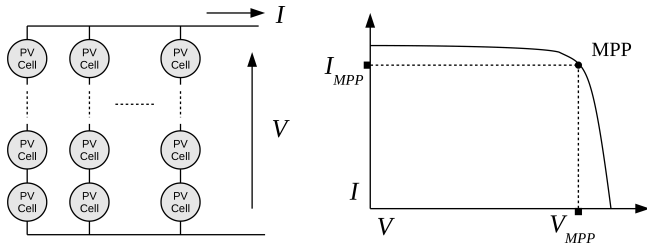


Fig. 4. I-V characteristics of PV-generator

The PV-devices are rated at Standard Test Conditions (STC: irradiance 1000 W/m^2 , spectrum AM1.5, temperature 25°C) and then MPP coordinates are referred to as nominal values: V_{MPPnom} , I_{MPPnom} and P_{MPPnom} . In order to generalize the discussion, all the PV voltages and current in the graphs have been normalized to the nominal values (MPP at STC) and shown in percent.

Since the PV-voltage depends logarithmically on irradiance, the interval of voltage change is relatively narrow. In field conditions of Central Europe, the MPP-voltage variations spans the range of only 15–20% of V_{MPPnom} .

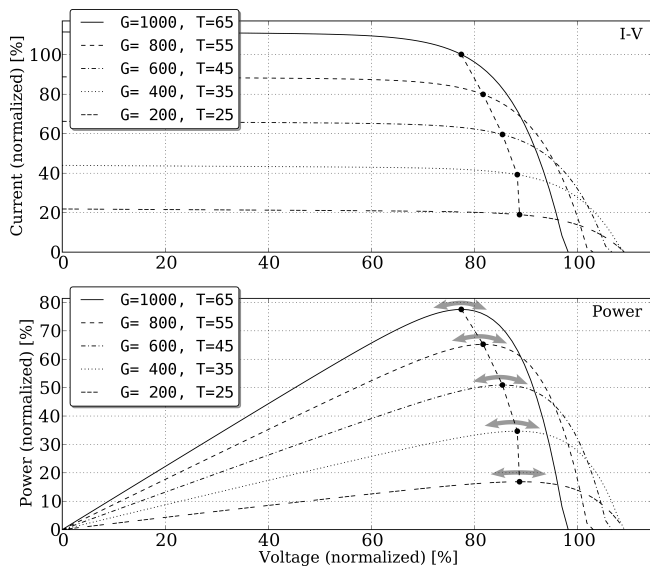


Fig. 5. PV-characteristics during sunny clear-sky day

During clear-sky days, the solar irradiance is changing slowly and is fairly stable in short terms. The MPP-transitions will be very slow and easy to follow, as shown in Fig. 5. High irradiance (G) and the cell temperature (T) will correspond to lower MPP-voltage and low irradiance – to higher one. The

tracking algorithm will oscillate around the true MPP, i.e. performing the operation of static tracking. Since the tracking is never perfect, some amount of offered solar energy will be lost.

However, during the rapid irradiance fluctuations due to passing clouds, the changes take place even within fraction of seconds and irradiance gradient can exceed $1000 \text{ W/m}^2/\text{s}$. Under such conditions, the transition of MPP can be treated as isothermal, as shown in Fig. 6, since thermal time constant of a PV-module is in order of minutes [7].

The MPP-tracking algorithm – in the best scenario – can follow the true MPP along the path indicated with top and bottom arrows (Fig. 6). This process of chasing a remote MPP is called a dynamic tracking. The mismatch between true MPP and actual operating point of PV-inverter may cause a significant energy losses in short terms.

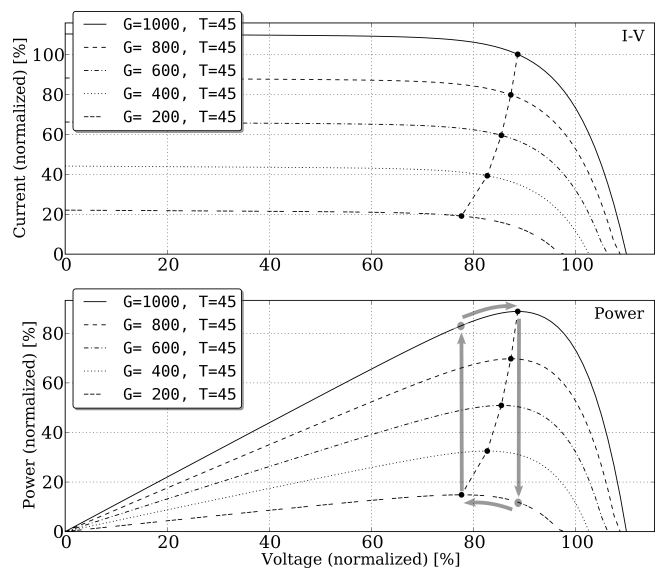


Fig. 6. PV-characteristics during rapid changes of irradiance

The effect of rapid transitions on energy efficiency is not symmetrical, though. The low-to-high irradiance transitions will cause higher power deviation from MPP and thus higher absolute energy losses as compared to high-to-low transitions. In both cases, the natural warming or cooling of the PV-panel just after the transition will slightly reduce the time to reach true MPP.

4. Efficiency of PV-inverter

In a small/medium PV grid-connected system, the utility grid can accept any amount of energy with no restrictions, in contrast to other storage methods or local loads, e.g. chemical batteries. In such a case the PV-system can achieve the highest energy conversion efficiency and the PV-inverter performance reflects the quality of its construction, including tracking abilities.

4.1. Efficiency definitions. In general, the only accurate record of the energy conversion efficiency η_E for any device,

is the ratio of its energy output (W_{AC}) to the input (W_{DC}), over a specified operating period:

$$\eta_{En} = \frac{W_{AC}}{W_{DC}}. \quad (1)$$

Energy efficiency is not very suitable for the inverter characterization, since the energy input is climate- and location-dependent. Instead, the power efficiency is used, defined as follows:

$$\eta_{DC/AC} = \frac{P_{AC}}{P_{DC}}, \quad (2)$$

where the instantaneous input and output power (P_{DC} , P_{AC}) must be averaged over 30 s to properly handle AC-signals, higher harmonics and DC-ripples, according to the standard [8]:

$$P_{AC \text{ or } DC} = \frac{1}{T} \int_0^T i(t)v(t)dt = \frac{1}{T} \int_0^T p(t)dt. \quad (3)$$

For long-term predictions, a single value of power efficiency can be misleading, especially if only a peak or rated efficiency is stated in manufacturer data sheets. On the other hand, the full efficiency vs. load curve is not convenient for the quantitative comparisons, either.

A solution – now widely adopted in industry – known as European efficiency η_{EU} , has been proposed as a weighted-sum of power efficiency for several load levels [9], as follows:

$$\eta_{EU} = 0.03\eta_{5\%} + 0.06\eta_{10\%} + 0.13\eta_{20\%} + 0.10\eta_{30\%} + 0.48\eta_{50\%} + 0.20\eta_{100\%}. \quad (4)$$

This expression can be relatively close to true energy efficiency, while still being a single-value parameter. Due to its definition, it cannot be accurate for different climatic conditions [10], but it is very suitable for overall devices comparison.

The inverter quality cannot be evaluated without studying the ability to maximize the PV output. The $\eta_{DC/AC}$ (or η_{EU}) describe only the essential DC/AC conversion, measured for stable DC input. The PV-inverters, however, operate with unstable DC input. Apart from DC/AC conversion, they must also track the position of MPP to capture the maximum energy offered by the PV-generator. The MPP-tracking process may lower the operation efficiency, without affecting $\eta_{DC/AC}$ itself.

The MPPT-efficiency can be defined as ratio of inverter DC input (P_{DC}) to maximum power (P_{MPP}) offered by the PV-generator:

$$\eta_{MPPT} = \frac{P_{DC}}{P_{MPP}}. \quad (5)$$

Finally, for very accurate inverter characterizations, the total efficiency (η_{total}) parameter has been proposed [11], comprising the two stages of energy processing:

$$\eta_{total} = \eta_{DC/AC} \cdot \eta_{MPPT} = \frac{P_{AC}}{P_{MPP}}. \quad (6)$$

The work is underway to establish a standard measurement procedure for η_{MPPT} with defined steepness and duration

of irradiance test pattern [12] suitable for future international standard.

4.2. MPP-tracking efficiency. The process of finding MPP can be considered separately for stable and varying irradiance, giving rise for two definitions of tracking efficiency: static and dynamic.

The static MPPT-efficiency ($\eta_{MPPT-Static}$) refers to the inverter operation under stable weather conditions. In this case the MPP position is fixed, but the tracking algorithm make the actual operating point to move around the true MPP. It can be expressed as:

$$\eta_{MPPT-Static} = \frac{\int_0^{t_M} v_{DC}(t)i_{DC}(t)dt}{P_{MPP}t_M}, \quad (7)$$

where v_{DC} , i_{DC} are measured for the inverter input, but the P_{MPP} is calculated for actual weather conditions and constant over the period t_M . The $\eta_{MPPT-Static}$ is usually around 99%, but there are evidences that it could be much worse [13, 14]. Taking into account that majority of electricity from PV is generated under stable conditions, even small improvements to $\eta_{MPPT-Static}$ are of importance.

Under highly variable irradiance (i.e. changing more than 100 W/m²/s), the deviation between inverter DC input and the true MPP grows. Finding the new MPP may last up to several seconds, depending on the tracking algorithm quality. The tracking efficiency during dynamic conditions ($\eta_{MPP-Dynamic}$) can be found according to:

$$\eta_{MPP-Dynamic} = \frac{\int_0^{t_M} v_{DC}(t)i_{DC}(t)dt}{\int_0^{t_M} p_{MPP}(t)dt}, \quad (8)$$

where the offered p_{MPP} is calculated for the transition period.

During variably cloudy days, that are common in Central and North Europe, the $\eta_{MPP-Dynamic}$ may be a non-negligible factor reducing the overall efficiency.

5. Tracking algorithms

In majority of solutions, the MPP-tracking is implemented as software algorithm, which controls the input impedance of DC/DC switched-mode converter of a PV-inverter. A review of control algorithms can be found in [15–17]. In general, the solutions can be classified as indirect or direct methods.

5.1. Indirect methods. The indirect (or quasi-see) algorithms conclude the location of MPP according to built-in knowledge and measurements of parameters other than P_{DC} . The built-in settings may include specific parameters of PV-generator, geographical location, climate features and meteorological measurements.

One example is a look-up table method, adjusting the V_{MPP} according to the actual irradiance and ambient temperature.

Another example is the “open-circuit voltage” method, which relies on approximately linear proportionality of V_{MPP} to V_{OC} (e.g. ~ 0.8 for crystalline silicon cells), setting the V_{MPP} periodically after taking samples of V_{OC} .

The main advantage of indirect methods is the ability to give the estimation of true MPP instantly. For some of them, a simplicity of control can be another asset.

The disadvantage for all the indirect methods is the need for tuning prior to the operation and the given MPP estimation may be of low accuracy, since they are insensitive to other phenomena such as aging or contamination.

5.2. Direct methods. The algorithms that rely on measurements of V_{DC} and I_{DC} (or P_{DC}) are called direct (or true-look) methods. They find the location of MPP iteratively, drawing conclusions from the previous samples. The MPP is approached by subsequent modifications of V_{DC} , making oscillations around the true MPP.

If the classification is done according to the decision-making logic, most of the algorithms fall into one out of two general categories: “hill-climbing” and artificial intelligence methods.

The “hill-climbing” algorithms exploit the known shape of the PV-power curve, climbing to the top from either the left or the right side. The best known examples include Perturb&Observe (P&O), Incremental Conductance (IC) methods and their variants.

The P&O algorithm computes the power difference ΔP in two consecutive measurements, resulting from the voltage perturbation by a constant ΔV . As long as ΔP is positive, the direction of voltage change is maintained, otherwise it is reversed. This leads to oscillations around true MPP and voltage drifts under rising irradiance. Many improvements to this basic scenario exist, however.

The IC method makes use of ΔV and ΔI . In contrast to P&O, the voltage change is done only when $\Delta I \neq 0$ is detected. After each perturbation ($+\Delta V$ for $\Delta I > 0$, $-\Delta V$ otherwise), the following condition for MPP is checked:

$$\frac{dP}{dV} = I + V \frac{dI}{dV} = 0 \Rightarrow -\frac{I}{V} = \frac{dI}{dV}. \quad (9)$$

Voltage modification is maintained ($+\Delta V$ for $dI/dV > -I/V$, $-\Delta V$ otherwise) until this condition is met, and then the modification are postponed. This way, the oscillations can be reduced and the drift eliminated.

The artificial intelligence methods, apart from direct measurements, make use of the past behavior of MPP. These include artificial neural networks, fuzzy logic, genetic algorithms and swarm chasing. It has been demonstrated that some improvement can be achieved, especially for hard-to-track cases of partial shading and irradiance changes conditions.

5.3. Application aspects. Despite so many variants of MPP-tracking algorithms, there is no consensus about superiority of any particular method. Apart from tracking efficiency, other criteria must be considered as well: complexity, speed, number of sensors, PV-system configuration, algorithm reliability

and sensitivity, and cost of implementation. The comparisons between different methods give different results since no universal framework for testing has been proposed.

The most widely used in commercial designs are the P&O and IC methods due to low cost and matured hardware implementations [16].

In both P&O and IC algorithms, the efficiency depends on tracking speed. This can be achieved either by bigger perturbation step or faster perturbation rate. The bigger step will result in increase of static tracking losses. On the hand, the faster rate is limited by measurement accuracy of signals with DC-ripples and speed of reaction to voltage perturbation in high power DC/DC converters [18].

5.4. Perturb&Observe The study in this article focuses on performance of P&O algorithm only. The method has been chosen for the simulation due to its wide application in commercial inverters.

The principle of P&O operation is shown in Fig. 7. It is worth noticing, that under stable conditions the oscillations can move the operation point further than one ΔV step.

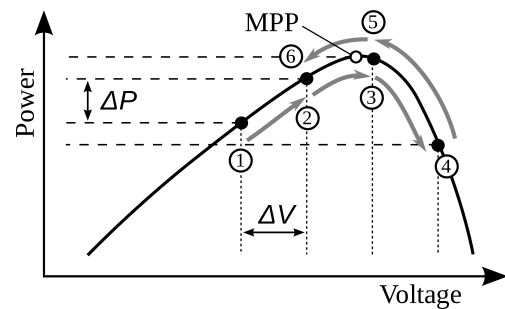


Fig. 7. P&O operation principle

In order to separately analyze the static and dynamic tracking process, the following criterion has been assumed for the inverter input voltage V_{DC} :

- $|V_{DC} - V_{MPP}| < 2\Delta V$: static tracking – the MPP can be reached (and step over) in less than two steps,
- $|V_{DC} - V_{MPP}| \geq 2\Delta V$: dynamic tracking – operation point is at least two steps away from MPP and the direction of voltage change will be maintained for at least three next steps.

The main drawback of P&O algorithm is the effect of voltage drift in the direction opposite to MPP, as shown in Fig. 8. Under increasing irradiance, the positive ΔP is detected regardless the search direction. The voltage can move significantly away, especially towards lower values due to lower slope of power curve.

The drift effect under decreasing irradiance is different, however. Since the ΔP becomes negative for a few consecutive steps, the direction of voltage change is altered every step. As a consequence, the operating point oscillates around the position of the last positive ΔP .

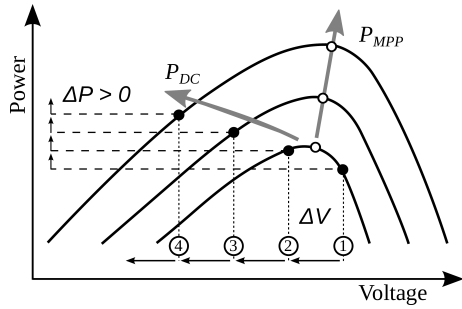


Fig. 8. Voltage drift in P&O under rising irradiance

Some improvements to the basic P&O have been proposed. For example a variable-time modifications [19] can reduce the drift and static oscillations but at a cost of speed. Another method called “three-point weight comparison” (TP-WC) [20] postulates to take the step backwards after positive ΔP in order to detect whether the rising irradiance contributed to ΔP . Both improvements slow down the operation speed and increase the complexity.

Both drift effects have negative influence on tracking performance. Longer step size will speed up the tracking, but also magnify the drift and magnitude of static oscillation. On the other hand, shorter steps may not be conclusive for flat parts of the power curve and will slow down the process. It is worth noticing, that in field conditions the location of MPP is almost never stable. The radiant flux, ambient temperature and cooling processes will constantly modify the I-V characteristics of PV-generator. According to the introduced criterion, all the tracking can be classified as dynamic or static when the step size becomes sufficiently small or long, respectively.

6. Simulation of MPP-tracking

The calculations has been performed for one-day data, June 2nd 2012 (Fig. 1) with highly variable irradiance, but by no means exceptional for the season, as shown in Fig. 2. The perturbation step, voltage and power of inverter input (ΔV , V_{DC} , P_{DC}) have been normalized to nominal (at STC) values (V_{MPPnom} and P_{MPPnom}).

6.1. Simulation model. The simulation of PV-generator has been done according to [6, 21] by solving numerically the convoluted equation of a single PV-module $I_m = f(V_m)$ for given cell temperature T_C and irradiance G at time points t throughout the simulated interval:

$$I_m = I_{Lm}(T_C(t), G(t)) - \frac{V_m - I_m R_{sm}}{R_{pm}} - I_{0m}(T_C(t)) \left[\exp \left(\frac{V_m - I_m R_{sm}}{V_{tm}(T_C(t))} \right) - 1 \right], \quad (10)$$

where the subscript m denotes the PV-module parameters: serial and shunt resistances R_{sm} and R_{pm} , photocurrent I_{Lm} and dark current I_{0m} .

The I_{Lm} and I_{0m} can be derived from I_{SCm} and V_{OCm} at STC, found in a PV-module data sheets, as follows:

$$I_{Lm}(T_C(t), G(t)) = (I_{SCm} + K_I \Delta T) \frac{G(t)}{G_{STC}}, \quad (11)$$

$$I_{0m}(T_C(t)) = \frac{I_{SCm} + K_I \Delta T}{\exp \left(\frac{V_{OCm} + K_V \Delta T}{a V_{tm}} \right) - 1}, \quad (12)$$

where $\Delta T = T_C(t) - T_{STC}$ refers to the temperature excess over nominal 25°C and G_{STC} is the nominal irradiance of 1000 W/m². The voltage and current temperature coefficients K_V and K_I have been assumed typical for crystalline silicon cells values of -0.5% and +0.05%, respectively. The diode ideality factor a is 1.5 and V_{tm} is the thermal voltage of serially connected cells in a module.

Together with electrical, the thermal simulation has been carried out according to single-section thermal RC-model. The thermal resistance R_{th} and capacitance C_{th} for a PV-module can be estimated or measured as shown in [7, 22]. The PV-cell temperature T_C in respect to ambient T_A and irradiance G has been found by solving the equation:

$$C_{th} \frac{dT(t)}{dt} + \frac{T(t)}{R_{th}} = G(t), \quad (13)$$

where $T(t) = T_C(t) - T_A(t)$ is the cell temperature excess above ambient. The time resolution for ambient temperature is 1 min.

The calculations have been performed for the 50 Wp PV-module *Solar-Fabrik SF 50A* using its electrical and thermal properties shown in Table 1. The thermal time-constant is about 5 minutes.

Table 1
PV-module parameters

cells	V_{OCm}	I_{SCm}	R_{sm}	R_{pm}	R_{th}	C_{th}
	[V]	[A]	[Ω]	[Ω]	[K/W m ²]	[J/K/m ²]
36	21.7	3.3	0.1	400	0.013	25800

Figure 9 shows a close-up of PV-cell temperature evolution. It is worth noticing, that under highly variable irradiance T_C cannot reach steady state due to the long time-constant of PV-modules and thus the location of MPP is constantly moving.

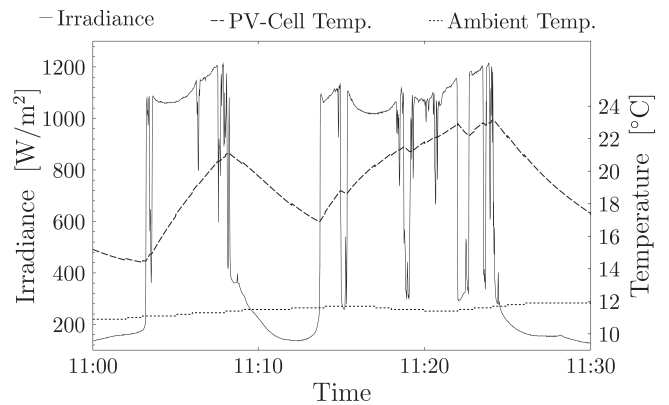


Fig. 9. Closeup of PV-module thermal response

6.2. Tracking operation close-up. In order to understand the final results better and verify the simulation correctness, several close-up pictures has been prepared. They present the behavior of important simulation variables for the period shown in Fig. 9.

Figure 10 demonstrates the imperfections of dynamic tracking operation. Too small ΔV is causing troubles to dynamic tracking, while the static tracking is almost perfect. The voltage drift is clearly visible for rising and dropping irradiance.

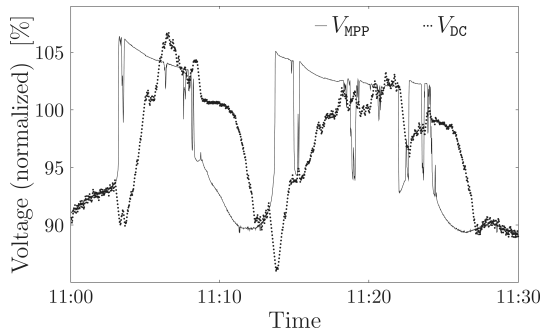


Fig. 10. Closeup of dynamic tracking ($\Delta V = 0.2\%$, $\Delta t = 1$ s)

When tracking step ΔV becomes too long, the static oscillations around MPP dominate the tracking operation, as shown in Fig. 11. The dynamic transitions, on the other hand, are handled much better, but the drift is unavoidable.

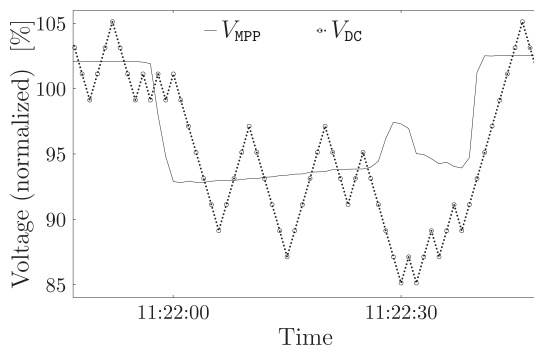


Fig. 11. Closeup of slow static tracking ($\Delta V = 2\%$, $\Delta t = 1$ s)

Since the value ΔV has the opposite influence on static and dynamic tracking, an optimal value of tracking step, with the best overall efficiency, can be expected.

6.3. Tracking efficiency close-up. Figure 12 shows the evolution of $\eta_{\text{MPPT-Dynamic}}$ in time, together with actual and available MPP-power. The deepest drop of efficiency always occurs for low-to-high irradiance transition and voltage drift at the same time. The instantaneous efficiency decrease may easily exceed 10% and this refers to the dynamic tracking only.

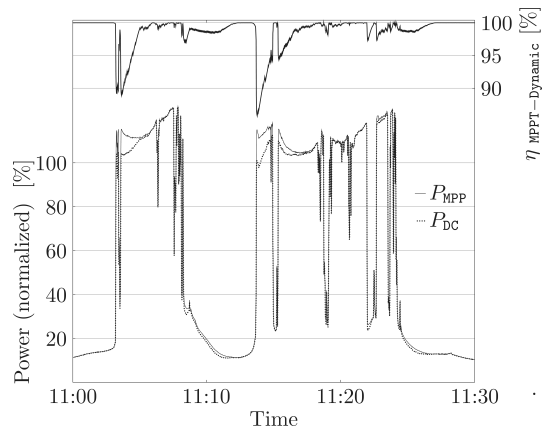


Fig. 12. Closeup of dynamic tracking efficiency ($\Delta V = 0.2\%$, $\Delta t = 1$ s)

The quality of static tracking is solely determined by the voltage perturbation magnitude. In intervals of fairly stable conditions, as shown in Fig. 13, the static efficiency is very high (above 99%), even for fairly large ΔV .

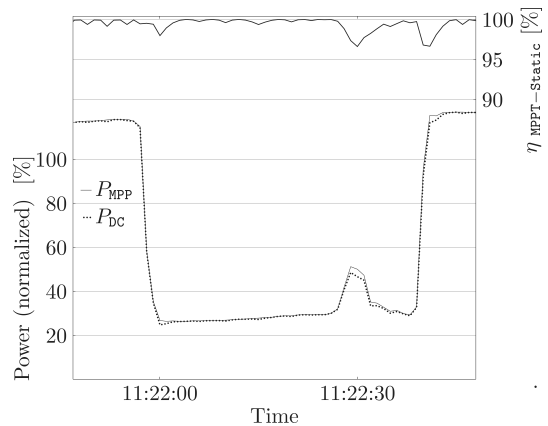


Fig. 13. Closeup of static tracking efficiency ($\Delta V = 2\%$, $\Delta t = 1$ s)

6.4. Results. The simulation of P&O algorithm has been carried out for:

- tracking rates Δt : 200 ms, 1 s, 2 s and 5 s,
- tracking steps ΔV : from 0.001% to 10% of V_{MPPnom} .

The results represent the energy received by PV-inverter with calculated static, dynamic and total tracking efficiency for June 2nd 2012 (Fig. 1).

Within the investigated interval, 6:00–20:00, there are over 250.000 time steps with 200 ms intervals. The simulation with high accuracy has been very time-consuming. A single-day tracking simulation requires the solution of convoluted PV-device equation that is embedded within optimization procedure to find P_{MPP} for each time step.

Figure 14 shows the daily amount of energy taken from the PV-generator in two tracking modes: static and dynamic, according to the before-mentioned classification. At the extreme sides almost all energy is handled under only one tracking mode: static for the biggest ΔV and dynamic for the

smallest. The energy corresponding to the tracking type that is not present for those extreme conditions would amount to zero.

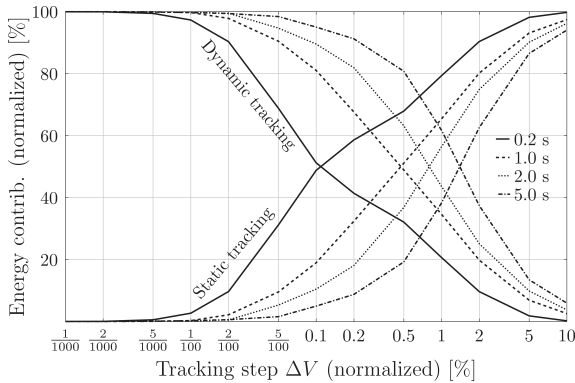


Fig. 14. Energy contribution delivered with static and dynamic tracking

The equal energy shares are obtained for different ΔV for various simulation rates Δt . However, when the voltage rate of change is considered, i.e. $\Delta V/\Delta t$, they all cross at approximately the value of 0.5 V%/s. These results suggest that the mode of tracking operation depends primarily on voltage change rate.

The static and dynamic tracking efficiency, for the investigated one-day period, are shown in Fig. 15. Static tracking performance is generally very high and falls down sharply only for voltage steps bigger than 5%, with little regard for the tracking rate.

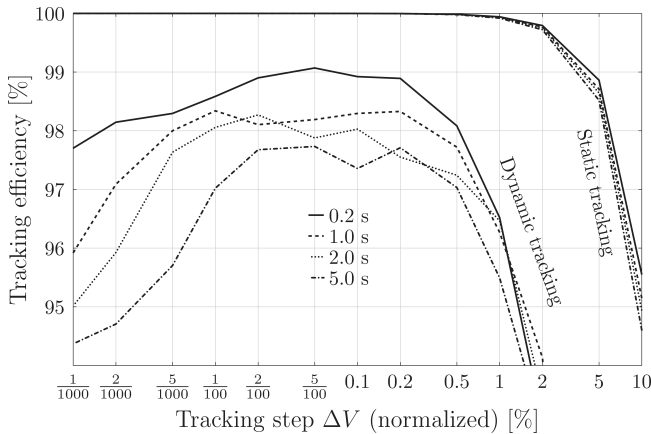


Fig. 15. Static and dynamic tracking efficiency

In contrast, the dynamic tracking is poor for both too small and too big voltage step, suffering from either too slow reaction or drift overshooting, respectively

The total tracking efficiency, in Fig. 16 is the resultant of static and dynamic ones, corrected for their energy contribution.

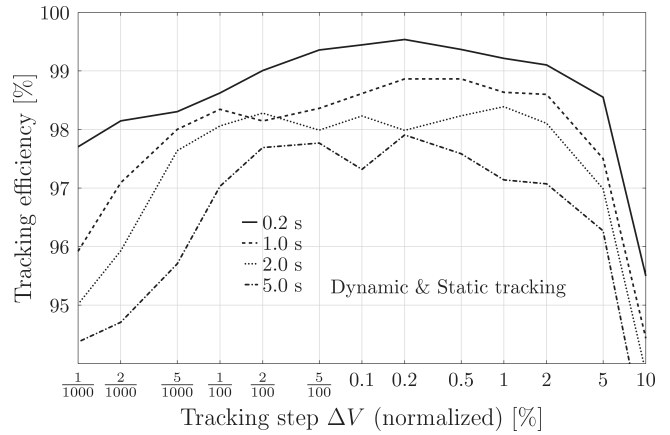


Fig. 16. Total tracking efficiency

A flat maximum can be found for tracking step ΔV between 0.02% to 2%. There is, however, a clear dependence on tracking rate. In general, faster rate always helps, but there may be technical limitations below value of 1 s. The rate slower than 2 s is not recommended as it lowers the efficiency by more than 2%.

7. Conclusions

Nowadays, the efficiency of modern PV-inverters for grid-connected systems is advertised as approaching 99%. While this may be true according to some measurements standards, the true energy efficiency over a longer period is always below the expectations.

The imperfect MPP-tracking is responsible for lower performance of the PV-inverter, without affecting its essential DC/AC conversion. This may be of importance especially under highly fluctuating sunshine, very common in Central and North Europe. It is now obvious, that the inverter quality cannot be evaluated without studying the tracking behavior.

The simulation in this paper has been aimed at studying the static and dynamic MPP-tracking efficiency for widely implemented P&O algorithm. In contrast to other studies on this subject, this work has the merit of using the high-quality irradiance data for Poland.

The calculations has been performed for a single variable-cloudy day representing the extreme, but very common, case of irradiance fluctuations. Therefore, the obtained results are setting the worst-case theoretical limits to the P&O tracking efficiency in Polish climate.

In response to fast irradiance changes, the unavoidable instantaneous power efficiency drops may exceed 10%, but during steady conditions the losses are kept below 1%, on the daily bases. The best results are expected for perturbation step between 0.2% and 2% of system nominal voltage. The fast rate of perturbation is generally favored, up to technical limits, and it should not be slower than 1–2 s.

The performance of field-installed inverters may still be worse as there is experimental evidence that handling this phenomenon is still not satisfactory and the problem deserves more attention.

REFERENCES

- [1] M.S. Imamura, P. Helm, and W. Palz, *Photovoltaic System Technology. A European Handbook*, H S Stephens & Associates, London, 1992.
- [2] T. Kozak, G. De Mey, A. De Vos, W. Marańda, and A. Napieralski, "Influence of ambient temperature on the amount of electric energy produced by solar modules", *Electronics, Technologies, Applications, SIGMA-NOT* 12, 46–48 (2009).
- [3] European Photovoltaic Industry Association, *Global Market Outlook For Photovoltaics 2013-2017, EPIA Report* (2013).
- [4] J. Kiciński, "Do we have a chance for small-scale energy generation? The examples of technologies and devices for distributed energy systems in micro & small scale in Poland", *Bull. Pol. Ac.: Tech.* 61 (4), 749–756 (2013).
- [5] W. Marańda, G. Jabłoński, and D. Makowski, "1 kWp PV System at Technical University of Lodz in Poland", *Proc. 19th Eur. PV Solar Energy Conf.* 3, 2915–2917 (2004).
- [6] M.G. Villalva, J.R. Gazoli, and E.R. Filho, "Comprehensive approach to modeling and simulation of photovoltaic arrays", *IEEE Trans. Power Electronics* 24 (5), 1198–1208 (2009).
- [7] W. Marańda and M. Piotrowicz, "Extraction of thermal model parameters for field-installed photovoltaic module", *Proc. 27th Int. Conf. on Microelectronics (MIEL)* 1 CD-ROM (2010).
- [8] *International Standard IEC 61683*, "Photovoltaic systems, Power conditioners, Procedure for measuring efficiency", 1999-11.
- [9] R. Hotopp, *Private Photovoltaik-Stromerzeugungsanlagen im Netzparallelbetrieb*, RWE Energie AG, Essen, 1990.
- [10] V. Salas, E. Olias, M. Alonso-Abella, and F. Chenlo, "Analysis between energy efficiency and european efficiency", *Proceedings of ISES Solar World Congress* 1, CD-ROM (2007).
- [11] H. Haeblerlin, L. Borgna, M. Kaempfer, and U. Zwahlen, "Total efficiency η_{TOT} – a new quantity for better characterisation of grid-connected PV inverters", *Proc. 20th Eur. PV Solar Energy Conf.* 1, CD-ROM (2005).
- [12] H. Haeblerlin and Ph. Schaerf, "New procedure for measuring dynamic MPP-tracking efficiency at grid-connected PV inverters", *24th Eur. PV Solar Energy Conf.* 1, CD-ROM (2009).
- [13] V. Salas, M. Alonso-Abella, F. Chenlo, and E. Olias, "Analysis of the maximum power point tracking in the photovoltaic grid inverters of 5 kW", *Renewable Energy* 34, 2366–2372 (2009).
- [14] M. Piotrowicz and W. Marańda, "Report on efficiency of field-installed PV-Inverter with focus on radiation variability", *Proceedings of Mixed Design of Integrated Circuits and Systems (MIXDES)* 1, CD-ROM (2013).
- [15] D.P. Hohmand and M.E. Ropp, "Comparative study of maximum power point tracking algorithms", *Progress in Photovoltaics: Research and Applications* 11 (1), 47–62 (2003).
- [16] N. Onat, "Recent developments in maximum power point tracking technologies for photovoltaic systems", *Int. J. Photoenergy* 2010 (245316), CD-ROM (2010).
- [17] V. Salas, E. Olias, A. Barrado, and A. Lazaro, "Review of the maximum power point tracking algorithms for stand-alone photovoltaic systems", *Solar Energy Materials & Solar Cells* 90, 1555–1578 (2006).
- [18] S. Pirog, R. Stala, and L. Stawiarski, "Power electronic converter for photovoltaic systems with the use of FPGA-based real-time modeling of single phase grid-connected systems", *Bull. Pol. Ac.: Tech.* 57 (4), 345–354 (2009).
- [19] N. Femia, G. Petrone, G. Spagnuolo, and M. Vitelli, "A technique for improving P&O MPPT performances of double-stage grid-connected photovoltaic systems", *IEEE Trans. on Industrial Electronics* 56, 11, 4473–4482 (2009).
- [20] C. Wang, M. Wu, S. Ou, K. Lin, and C. Lin, "Analysis and research on maximum power point tracking of photovoltaic array with fuzzy logic control and three-point weight comparison method", *Science China Technological Sciences* 53 (8), 2183–2189 (2010).
- [21] W. Marańda, "Numerical modeling of photovoltaic devices with python scripting language", *Proc. 17th Int. Conf. on Information Technology Systems* 1, CD-ROM (2010).
- [22] G. De Mey, J. Wyrzutowicz, A. De Vos, W. Marańda, and A. Napieralski, "Influence of lateral heat diffusion on the thermal impedance measurement of photovoltaic panels", *Solar Energy Materials and Solar Cells* 112, 1–5 (2013).